J Pharmacokinet Pharmacodyn (2008) 35:285–323
DOI 10.1007/s10928-008-9089-1

Modeling time variant distributions of cellular lifespans: increases in circulating reticulocyte lifespans following double phlebotomies in sheep

Kevin J. Freise · John A. Widness · Robert L. Schmidt · Peter Veng-Pedersen

Received: 31 October 2007 / Accepted: 18 April 2008 / Published online: 14 June 2008

Abstract Many pharmacodynamic (PD) models of cellular response assume a single and time invariant lifespan of all cells, despite the existence of a true underlying distribution of cellular lifespans and known changes in the lifespan distributions with time. To account for these features of cellular populations, a time variant cellular lifespan distribution PD model was formulated and theoretical aspects of modeling cellular populations presented. The model extends prior work assuming time variant "point distributions" of cellular lifespans (Freise et al. J Pharmacokinet Pharmacodyn 34:519–547, 2007) and models assuming a time invariant lifespan distribution (Krzyzanski et al. J Pharmacokinet Pharmacodyn 33:125–166, 2006). The formulated time variant lifespan distribution model was fitted to endogenous plasma erythropoietin (EPO), reticulocyte, and red blood cell (RBC) concentrations in sheep phlebotomized on two occasions, 8 days apart. The time variant circulating reticulocyte lifespan was modeled as a truncated and scaled Weibull distribution, with the location parameter of the distribution non-parametrically represented by an end constrained quadratic spline function. The formulated time variant lifespan distribution model was compared to the identical time invariant distribution, time variant "point distribution", and time invariant "point distribution" cellular lifespan models. Parameters of the time variant lifespan distribution model were well estimated with low standard errors. The mean circulating reticulocyte lifespan was estimated at 0.304 days, which rapidly increased over 3-fold following the first phlebotomy to a maximum of 1.03 days ($P = 0.009$).

Prepared for submission to *Journal of Pharmacokinetics and Pharmacodynamics*.

K. J. Freise · P. Veng-Pedersen (✉)
College of Pharmacy, The University of Iowa, 115 S. Grand Ave., Iowa City, IA 52242, USA
e-mail: veng@uiowa.edu

J. A. Widness · R. L. Schmidt
Department of Pediatrics, College of Medicine, The University of Iowa, Iowa City, IA 52242, USA

On average, the percentage of erythrocytes being released as reticulocytes maximally increased an estimated two-fold following the phlebotomies. The primary features of immature RBC physiology were captured by the model and gave results consistent with other estimates in sheep and humans. The comparison of the four lifespan models gave similar parameter estimates of the stimulation function and fits to the RBC data. However, the time invariant models fit the reticulocyte data poorly, while the time variant "point distribution" cellular lifespan model gave physiologically unrealistic estimates of the changes in the circulating reticulocyte lifespan under stress erythropoiesis. Thus the underlying physiology must be considered when selecting the most appropriate cellular lifespan model and not just the goodness-of-fit criteria. The proposed PD model and the numerical implementation allows for a flexible framework to incorporate time variant lifespan distributions when modeling populations of cells whose production or stimulation depends on endogenous growth factors and/or exogenous drugs.

Keywords Pharmacokinetics · Erythropoiesis · Anemia · Time variant kinetics · Mean potential lifespan · Survival analysis · Cellular transformations · Hematology · Blood cells · Systems analysis · Convolution

Introduction

Determination of the lifespan distributions of cells has been an interest to researchers for many years. Some of the first work determined the lifespans of red blood cells from cell survival curves [1–3]. However, much of the early work assumes constant production rates and distributions of cellular lifespans. With the development of many new drugs that affect important cell populations, such as cancerous, erythrocyte, leukocyte, platelet, and bacterial cell populations, the study of the effect of these new drugs on both the production and destruction is an important consideration for optimal dosing. For cell death mechanisms that are related to the age of the cell, i.e., time since production, the lifespan distributions and age structure of the population are vitally important for understanding the effect of the therapeutic agent.

With respect to red blood cells (RBC), under non-disease state conditions the mechanism of cell death is primarily due to cellular senescence (i.e., the expiration of the cellular lifespan) [4]. The two primary RBC types in the systemic circulation are reticulocytes and mature erythrocytes, the former which is just an immature RBC. Reticulocytes are produced from erythroid progenitor cells located primarily in the bone marrow, where they initially reside and subsequently are released from into the systemic circulation [5]. The maturation of erythroid progenitor cells into reticulocytes and ultimately RBCs is primarily controlled by erythropoietin (EPO), a 35 kD glycoprotein hormone produced by the pertibular cells of the kidney in response to oxygen need [5]. During the development from erythroid progenitor cells their hemoglobin content increases until it develops into a reticulocyte upon nucleus extrusion, where further maturation primarily involves the removal of ribosomal RNA, remodeling of the plasma membrane, and a progressive decrease in cell size [5–7].

In humans the majority of the erythrocytes released from the bone marrow into the systemic circulation are reticulocytes, while in other species such as ruminants and horses, under basal erythropoietic conditions (i.e., non-anemic or non-erythropoietically stimulated) the majority of the erythrocytes are released as mature RBC's [6–8]. In general, under basal erythropoietic conditions in humans, reticulocytes have a lifespan in the systemic circulation of approximately 24 h before developing into mature RBCs. However, during stress erythropoiesis (i.e., stimulated erythropoietic conditions), the reticulocyte lifespan in the circulation increases to an estimated 2–3 days [9]. In humans, the reticulocytes produced under stress erythropoiesis also contain more residual ribosomal RNA, are larger, and have less flexible plasma membranes than those produced under normal basal conditions, and therefore are thought to be immature reticulocytes that under "normal" physiological conditions reside in the bone marrow until being released as more mature reticulocytes [7,9–11]. Similarly in animals such as ruminants with a low basal percentage of erythrocytes released as reticulocytes, the percentage of reticulocytes increases dramatically during stress erythropoiesis [8,12]. Therefore like humans, younger erythrocytes are also released following stress erythropoiesis in these species. Accordingly, the reticulocyte counts increase under stress erythropoiesis not only due to increased reticulocyte production in response to EPO stimulation, but also due to a longer lifespan in the systemic circulation.

One of the most common techniques for modeling the pharmacokinetic/pharmacodynamic (PK/PD) relationship between therapeutic agents, such as EPO, and the cellular populations is the compartmental or cellular "pool" model, in which cells are transferred between compartments by first-order processes [13]. A major limitation of this model is that it completely ignores the age structure of cells within a compartment, treating all cells within the compartment as equally likely to be transferred out of the compartment. For cells like reticulocytes and mature erythrocytes whose "removal" from the sampling compartment is primarily determined by a developmental processes (i.e., transformation into a mature RBC) and cellular senescence, respectively, more physiologically realistic models incorporate a cellular lifespan component [14–21]. However, nearly all of these PK/PD models assumed a single "point distribution" of cellular lifespans shared by all cells that does not vary over time (i.e., time invariant). More recently, models have been introduced that account for a *time invariant* distribution of cell lifespans [22] and *time variant* "point distributions" of cellular lifespans [23].

To date, a PD cellular response model that incorporates a *time variant* distribution of cellular lifespans has not been presented and successfully fitted to data. Additionally, a time variant distribution of reticulocyte lifespans has not been described following induction of stress erythropoiesis conditions, nor have estimates of changes in the proportion of erythrocytes released as reticulocytes and mature RBCs been previously obtained. Therefore, the objectives of the current work were: (1) to present a general PD model that incorporates a time variant distribution of cellular lifespans, (2) to successfully fit the presented model to erythrocyte data following stress erythropoiesis to estimate the changes in the circulating reticulocyte lifespan and proportion of erythrocytes released into the systemic circulation as reticulocytes, and (3) to compare the presented model to other cellular lifespan models.

Theoretical

Time variant cellular disposition

Let $\ell(\tau, z)$ denote the *time variant* probability density function (p.d.f.) of cellular lifespans, where τ is the cellular lifespan and z is an arbitrary time of production (Fig. 1a). More specifically, the cellular lifespan is defined for a particular cell type of interest the time from input into the sampling space to the time of output from the sampling space, which may be due to: cellular death/senescence, transformation into a different cell type, and/or irreversible removal from the sampling space. Therefore, the lifespan of a cell is determined by the definition of both the cell type and the sampling space. Under the above definition of cellular lifespan it could also be described as the residence time in the sampling space of the cell type of interest. Additionally, cellular production is defined as the physical input of cells into the sampling space. Let it be assumed that at the time of production each cell is assigned a unique lifespan which is not further affected by subsequent environmental conditions following production. Therefore, the z variable references the lifespan distribution to the particular time of production. Since it is assumed that after production the lifespan of the cells is not affected by the environment, the cells act independent of each other following entry into the sampling space and therefore have a linear cellular disposition [23]. Due to the above properties, each cell is assigned an individual probability of survival after production that may vary with the time of production. The probability of cellular survival to a particular time t after production is given by the time variant unit response (UR_ℓ) function [23], which can also be viewed as a survival function from failure time data analysis [24]. Accordingly:

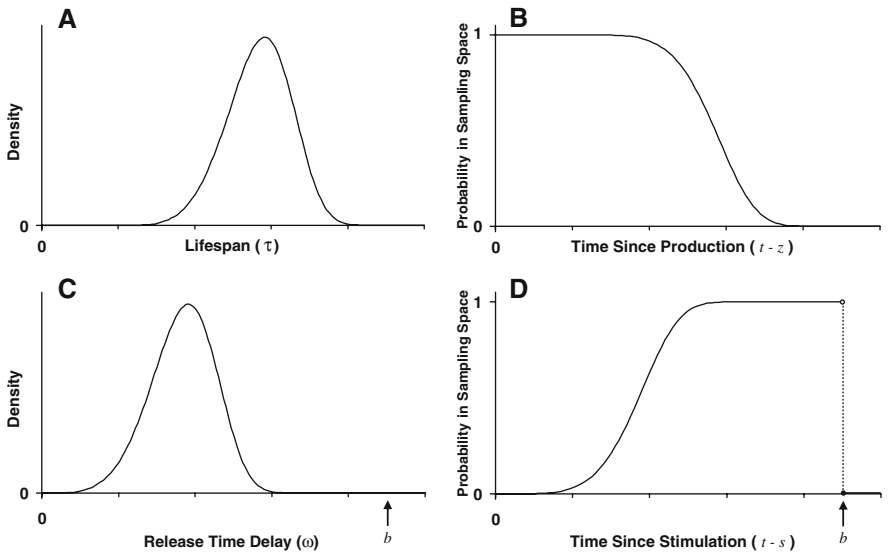

Fig. 1 Illustration of the relationship between the time variant lifespan distribution, $\ell(\tau, z)$ (**a**), and the corresponding unit response, $UR_\ell(t, z)$, from Eq. 3 (**b**) and the relationship between the time variant release time delay distribution, $r(\omega, s)$ (**c**), and the corresponding unit response, $UR_r(t, s)$, from Eq. 8 (**d**)

$$UR_\ell(t,z) = P(\mathrm{T} > t-z, z) = \int_{t-z}^{\infty} \ell(\tau, z)\, d\tau = 1 - \int_{0}^{t-z} \ell(\tau, z)\, d\tau, \quad t \geq z \quad (1)$$

where t is the current time, $P(\cdot)$ denotes the probability, and T denotes a random cellular lifespan variable. Therefore the UR_ℓ is the cellular disposition, as illustrated in Fig. 1b. Let $f_{prod}(t)$ denote the production (i.e., input) rate of cells into the sampling space, which is typically a function of time through endogenous growth factors and/or exogenous drug, and let Δz denote a small time increment. Then the number of cells currently present in the sampling space at time t that were produced at a previous time z is given by the product of the number of cells produced at time z and the probability that these cells have survived to time t (i.e., $UR_\ell(t,z)$):

$$f_{prod}(z) \cdot \Delta z \cdot UR_\ell(t,z) \quad (2)$$

Summation of Eq. 2 by integration across all time prior to t followed by substitution of Eq. 1 into the resulting equation gives the *general key equation* for the total number of cells in the current sampling space population when modeling a time variant cellular lifespan distribution:

$$\begin{aligned} N(t) &= \underset{\Delta z \to 0}{limit} \sum_{Z:z\leq t} f_{prod}(z) \cdot \Delta z \cdot UR_\ell(t,z) = \int_{-\infty}^{t} f_{prod}(u) \cdot UR_\ell(t,u)\, du \\ &= \int_{-\infty}^{t} f_{prod}(u) \cdot \left[1 - \left[\int_{0}^{t-u} \ell(\tau, u)\, d\tau\right]\right] du \end{aligned} \quad (3)$$

As can be observed from Eq. 3, the number of cells in the sampling space is given by an integral of the product of the number of cells produced at a previous time and the probability that the cells produced at that previous time are present in the sampling space at the current time. The lower integration limit of $-\infty$ in Eq. 3 is to be interpreted to consider "all prior history" of the system that affects $N(t)$. Due to the finite lifespan of cells, in reality the lower limit may be explicitly stated as t minus the maximal cellular lifespan, if known. Differentiation of Eq. 3 results in:

$$\frac{dN}{dt} = f_{prod}(t) - \int_{-\infty}^{t} f_{prod}(u) \cdot \ell(t-u, u)\, du \quad (4)$$

as previously presented [20]. Thus the input rate into sampling space at time t is given by $f_{prod}(t)$ and the output rate from the sampling space is given by $\int_{-\infty}^{t} f_{prod}(u) \cdot \ell(t-u, u)\, du$.

Accounting for subject growth

Measurement of cells in vivo is often done in terms of concentrations, $C(t)$, such as number of reticulocytes per volume of blood, therefore, Eq. 3 is divided by the total sampling space volume, $V(t)$, resulting in:

$$C(t) = \frac{N(t)}{V(t)} \tag{5}$$

If the subject is mature or the observation time window/cell lifespans are short relative to the rate of change in the sampling space volume, then $V(t)$ can reasonably be assumed to be constant, simplifying Eq. 5. However, if the subject is growing, and therefore the sampling space volume is changing with time, and the time window and/or cell lifespan is relatively long, the dilution of the cellular concentration due to volume expansion must be considered.

Corrections for cell removal

To improve the analysis of the cell population it is necessary to correct for the effect of external removal of cells, such as a phlebotomy. Let f denote the fraction of cells remaining immediately following a phlebotomy conducted at time t_P, then to correct for a phlebotomy when $t \geq T_P$ Eq. 3 simply becomes (see Appendix A):

$$\begin{aligned} N(t) = F \cdot \int_{-\infty}^{T_P} f_{prod}(u) \cdot \left[1 - \left[\int_0^{t-u} \ell(\tau, u)\, d\tau\right]\right] du \\ + \int_{T_P}^{t} f_{prod}(u) \cdot \left[1 - \left[\int_0^{t-u} \ell(\tau, u)\, d\tau\right]\right] du, \quad t \geq T_P \end{aligned} \tag{6}$$

Calculation of the sampling space volume

By the external removal or addition of cells to the sampling space, the volume of the sampling space can be estimated under the assumption that the total sampling space volume remains constant. Following an acute phlebotomy (i.e., removal of blood cells) the original blood volume is re-established within 24–48 h if no plasma volume expanders are administered [7,25], therefore the assumption of a constant blood volume (i.e., the sampling space) is reasonable when dealing with populations of blood cells and the 24–48 h lag-time for re-establishment of the blood volume is considered. The original blood volume will be reestablished even more rapidly if plasma or other blood volume expander is administered, due to increased osmotic pressure in the vascular system. In case of an acute removal or addition of cells, the sampling space volume is given by:

$$V(T_P) = \frac{N_P}{\Delta C} \tag{7}$$

where N_P denotes the number of cells removed or added and ΔC denotes the magnitude of the change in the cell concentration due to the phlebotomy or transfusion, respectively. In the case of a transfusion, the additional assumption must also be made that a substantial fraction of the transfused cells are not rapidly removed from the sampling space, such as spleenic removal of transfused RBCs from the systemic circulation due to damage that occurred during the storage or transfusion process.

Alternative parameterization of a time variant cellular disposition

For many populations of cells there is a time delay between the activation or stimulation of cells and the physical input of the stimulated cells into the sampling space. An example is stimulation of erythroid precursor cells in the bone marrow (i.e., outside the sampling space) and the subsequent release of the stimulated cells into the systemic circulation (i.e., the sampling space) as either reticulocytes or mature RBCs. In this instance a time variant cellular lifespan can be alternatively parameterized as follows. Let the time of cellular stimulation be denoted by s and let ω denote the time delay from cellular stimulation to appearance or release of the subsequently stimulated cell(s). Then a time variant cellular disposition can be accounted for by assuming the time delay of the release of a cell to be a random variable and the time from stimulation of the cell to the time of output from the sampling space to be a fixed period of time, denoted b. As before, the output from the sampling space may be due to cellular death/senescence, transformation into a different cell type, and/or irreversible removal. Let $r(\omega, s)$ denote a time variant p.d.f. of release time delays into the sampling space (Fig. 1c). Then the probability that a cell is present in the sampling space as the cell type of interest is given by the intersection of the events that the time since stimulation is less than b and that the cell has been released into the sampling space. In this instance let it also be assumed that the probability of these two events are independent of each other and that at the time of stimulation each cell is assigned a unique release time delay which is not further affected by subsequent environmental conditions following stimulation; thus the cells act independent of each other following stimulation and have a linear cellular disposition. Therefore, the probability that a cell resulting from progenitor cell stimulation at time s is present in the sampling space at time t can be defined in terms of a unit response of the cell type of interest, denoted UR_r (Appendix B), and is given by:

$$\begin{aligned} UR_r(t,s) &= 1\{t-s<b\}\cdot P(\Omega \le t-s, s) \\ &= [1-U(t-s-b)]\int_0^{t-s} r(\omega,s)\,d\omega, \quad t \ge s \end{aligned} \tag{8}$$

where $1\{X\}$ is the indicator function which is equal to 1 if X is true and 0 otherwise, Ω is a random release time delay variable, and u is the unit step function described by:

$$U(\mathbf{x}) = \begin{cases} 1 & \text{if } x \geq 0 \\ 0 & \text{otherwise} \end{cases} \tag{9}$$

It can be observed from Eq. 8 and Fig. 1d, if $\omega \geq b$ then the UR_r has a value of 0, as logically expected. If not all the cells stimulated at time s have been released yet by time b, then an UR_r value of 0 can be interpreted as a fraction of the cells died prior to release into the sampling space and/or a fraction of the cells transformed into a different cell type prior to release.

Let $f_{stim}(t)$ denote the stimulation rate of cells, then similar to Eq. 3 the number of cells in the population is given by integration across all prior time of the product of $f_{stim}(t)$ and Eq. 8:

$$\begin{aligned} N(t) &= \int_{-\infty}^{t} f_{stim}(u) \cdot \left[[1 - U(t-u-b)] \cdot \int_{0}^{t-u} r(\omega, u)\, d\omega \right] du \\ &= \int_{t-b}^{t} f_{stim}(u) \cdot \left[\int_{0}^{t-u} r(\omega, u)\, d\omega \right] du \end{aligned} \tag{10}$$

which is the analogous equation to Eq. 3. The unit step function is eliminated in the simplification step of Eq. 10 since it is recognized that the integrand will have a value of 0 at all times when $u < t - b$. Similar to Eqs. 3 and 6, a correction for a phlebotomy is needed for Eq. 10 when the time interval from $t - b$ to t contains T_P (i.e., contains a phlebotomy). During this time interval the equation for $N(t)$ (Appendix C) then becomes:

$$\begin{aligned} N(t) = &\int_{t-b}^{t} f_{stim}(u) \cdot \left[\int_{0}^{t-u} r(\omega, u)\, d\omega \right] du \\ &- [1 - F] \cdot \int_{t-b}^{T_P} f_{stim}(u) \cdot \left[\int_{0}^{T_P - u} r(\omega, u)\, d\omega \right] du, \quad t - b < T_P \leq t \end{aligned} \tag{11}$$

The p.d.f.'s $\ell(\tau, \cdot)$ and $r(\omega, s)$ are related by the expression:

$$\ell(\tau, s) = \begin{cases} \frac{r(b-\tau, s)}{\int_0^b r(\omega, s)\, d\omega} & \text{if } 0 \leq \tau < b \\ 0 & \text{otherwise} \end{cases} \tag{12}$$

as derived in Appendix D. The p.d.f. $\ell(\tau, \cdot)$ is now indexed by s instead of z, as the time of stimulation is when the unit response was defined for a cell. As can be observed from Eq. 12, a time variant cellular lifespan is still being modeled by considering the release time delay from stimulation to release to be a random variable with a fixed time period between stimulation and output from the sampling space of the subsequently released cell.

Materials and methods

Animals

All animal care and experimental procedures were approved by the University of Iowa Institutional Animal Care and Use Committee. Four healthy young adult sheep approximately 4 months old and weighing 23.5 (1.14) kg (mean (SD)) at the beginning of the experiment were utilized. Animals were housed in an indoor, light- and temperature-controlled environment, with ad lib access to feed and water. Prior to study initiation, jugular venous catheters were aseptically placed under pentobarbital anesthesia. Intravenous ampicillin (1 g) was administered daily for 3 days following catheter placement.

Study protocol

Blood samples (∼0.5 ml/sample) for plasma EPO, reticulocyte counts, and RBC determination were collected for 5–12 days to determine baseline values prior to conducting the first of two controlled phlebotomies over several hours to induce acute anemia. The second phlebotomy was conducted 8 days later. For each phlebotomy, animals were phlebotomized to hemoglobin concentrations of 3–5 g/dl. To maintain a constant blood volume during the procedure, the plasma removed during the phlebotomy was collected and infused back into the animal. Additionally, a volume 0.9% NaCl solution was infused so that a 1-to-1 total volume of fluid exchange was conducted during each phlebotomy. The total number of RBCs removed at each phlebotomy was determined by assaying a sample of the removed volume. Blood samples were collected 1–4 times daily between the phlebotomies and for 15–42 days following the second phlebotomy. Animal weights were also recorded upon study initiation and 1–2 times weekly throughout the course of the experiments. No iron supplementation other than that in the animal's feed was given. To minimize erythrocyte loss due to frequent blood sampling, blood was centrifuged, the plasma for EPO determination removed, and the unused red cells re-infused.

Sample analysis

Plasma EPO concentrations were measured in triplicate using a double antibody radioimmunoassay (RIA) procedure as previously described (lower limit of quantitation 1 mU/ml) [26]. All samples from the same animal were measured in the same assay to reduce variability. The reticulocyte and RBC counts were determined using the ADVIA® 120 Hematology System (Bayer Corp., Tarrytown, NY). In total, for each subject approximately 40–50 samples were analyzed for erythrocyte counts and 50–100 samples were analyzed for plasma EPO determination.

Specific model formulation

Erythropoietin was considered to be the stimulator of the erythroid cell precursors. The stimulation rate was related to the plasma EPO concentration (C_P) with time using a systems analysis approach that focuses on their overall functional relationship

[27]. A biophase conduction function and a Hill equation transduction function were utilized, specifically, the biophase concentration (C_{bio}) was determined by:

$$C_{bio}(t) = k_{bio} \cdot \exp(-k_{bio} \cdot t) * C_P(t) \tag{13}$$

where '$*$' denotes the convolution operator and k_{bio} is the biophase conduction function parameter. For $t \leq t_0$, C_P was set to the initial (first observation) fitted plasma EPO concentration (i.e., steady-state plasma EPO concentration assumption). The EPO plasma concentrations were non-parametrically represented using a generalized cross validated cubic spline function [28], and the convolution of the fitted cubic spline with the conduction function given in Eq. 13 was analytically determined. The stimulation rate was subsequently related to C_{bio} by the transduction function given by:

$$f_{stim}(t) = \frac{E_{max} \cdot C_{bio}(t)}{EC_{50} + C_{bio}(t)} \cdot m(t) \tag{14}$$

where f_{stim} is the redefined stimulation function from Eq. 10 that depends on $C_{bio}(t)$ and the animal mass, $m(t)$, E_{max} is the maximal erythrocyte (RBC) stimulation rate in cells/kg/day, and EC_{50} is the biophase EPO concentration that results in 50% of maximal erythrocyte stimulation rate (E_{max}). The mass of the animal was incorporated into the model to account for subject growth prior to and during the experiment, as it is likely that the total mass of erythrocytes produced (stimulated) would increase with growth as the erythropoietic progenitor cell mass increases. As with the stimulation rate, proportionality between blood volume and animal mass was assumed to account for growth induced blood volume expansion during the experiment, as given by:

$$V(t) = V_{\mathrm{n}} \cdot m(t) \tag{15}$$

where V_{n} is the mass normalized constant total blood volume. Hence the modeled sampling space is defined as the total blood volume of the systemic circulation. Due to the relatively young age and rapid growth of lambs, the animal mass, $m(t)$, was represented as a monoexponential fit to the animal weight data as given by:

$$m(t) = A \cdot \exp(\alpha \cdot [t - t_0]) \tag{16}$$

where A is the body mass (weight) at time t_0 and α is a first-order growth rate constant.

The release time delay p.d.f., $r(\omega, s)$, from Eq. 10 was modeled as a Weibull distribution due to the flexibility of the distribution, its support on the non-negative real line, and the analytical solution to its cumulative distribution function. Specifically:

$$r(\omega, s) = \begin{cases} \frac{k}{\lambda} \cdot \left[\frac{\omega - \theta(s)}{\lambda}\right]^{k-1} \cdot \exp\left(-\left[\frac{\omega - \theta(s)}{\lambda}\right]^{k}\right) & \text{for } \omega \geq \theta(s) \text{ and } 0 \leq \omega < \infty \\ 0 & \text{otherwise} \end{cases} \tag{17}$$

with:

$$\lambda > 0, \quad k > 0, \text{ and } \theta(s) \geq 0 \text{ for all } s$$

where λ, k, and $\theta(s)$ are the scale, shape, and location parameters, respectively, with only the location parameter being time variant. From Eq. 8 to Eq. 17 it follows that:

$$\int_0^{t-s} r(\omega, s)\, d\omega = \begin{cases} 1 - exp\left(-\left[\frac{t-s-\theta(s)}{\lambda}\right]^k\right) & \text{for } t-s \geq \theta(s) \text{ and } 0 \leq t-s < \infty \\ 0 & \text{otherwise} \end{cases} \tag{18}$$

The time variance of the distribution was assumed to enter through the location parameter due to the simplicity of the interpretation in changes of $\theta(s)$. However, the presented model and the numerical implementation (see below) readily extends time variance in the other distribution parameters.

To account for the double phlebotomies, let T_{P1} and T_{P2} be defined as the time of the first and second phlebotomy, respectively, and let F_1 and F_2 be the corresponding fraction of the cells remaining after the phlebotomy. Then from extensions of Eq. 11 to two phlebotomies (Appendix E), the number of cells present at time t is given by:

$$\begin{aligned} N(t) = & \int_{t-b}^{t} f_{stim}(u) \cdot \left[\int_0^{t-u} r(\omega, u)\, d\omega\right] du - U(t - T_{P1}) \cdot [1 - F_1] \\ & \cdot \int_{min(T_{P1}, t-b)}^{T_{P1}} f_{stim}(u) \cdot \left[\int_0^{T_{P1}-u} r(\omega, u)\, d\omega\right] du \\ & - U(t - T_{P2}) \cdot [1 - F_2] \cdot \int_{min(T_{P2}, t-b)}^{T_{P2}} f_{stim}(u) \cdot \left[\int_0^{T_{P2}-u} r(\omega, u)\, d\omega\right] du \\ & + U(t - T_{P2}) \cdot [1 - F_2] \cdot [1 - F_1] \cdot \int_{min(T_{P1}, t-b)}^{T_{P1}} f_{stim}(u) \\ & \cdot \left[\int_0^{T_{P1}-u} r(\omega, u)\, d\omega\right] du \end{aligned} \tag{19}$$

with:

$$F_i = 1 - \frac{N_{Pi}}{N(T_{Pi} - \varepsilon)}, \quad i = 1, 2 \tag{20}$$

where $min(T_{Pi}, t - b)$ is the minimum of T_{Pi} and $t-b$, $f_{stim}(u)$ is given by Eq. 13 and Eq. 14, and $\int_0^{t-u} r(\omega, u)\, d\omega$ is given by Eq. 18. Additionally, ε denotes an infinitely small time increment and N_{P1} and $N_{P2}$the number of cells removed by the first and second phlebotomy, respectively. The fraction of cells remaining after a phlebotomy

will be the same for both reticulocytes and RBCs, and therefore only a single F_1 and F_2 is calculated for both populations of cells. For $t \leq t_0$, the release time delay distribution was assumed to remain at the initial (t_0) release time delay distribution (i.e., $r(\omega, s) = r(\omega, t_0)$ for $s \leq t_0$). An end-constrained quadratic spline function was used to non-parametrically estimate the Weibull distribution time variant location parameter (i.e., $\theta(s)$) of the release time delay distribution, as further detailed in Appendix F.

Specifically, let the time from stimulation of a erythroid precursor cell to transformation of the subsequently stimulated reticulocyte (either in the marrow or systemic circulation) into a mature RBC be denoted as b_{RET} and the time from stimulation of a erythroid precursor cell to senescence/destruction of the subsequently stimulated RBC (immature + mature) be denoted as b_{RBC}. Due to the fact that a reticulocyte is an immature RBC, then replacement of b by b_{RET} or b_{RBC} in Eq. 19 gives the fitted equation for the number of reticulocytes ($N_{RET}(t)$) or the number of RBCs ($N_{RBC}(t)$), respectively. The modeled relationship between $r(\omega, s)$, b_{RET}, and b_{RBC} is schematically illustrated in Fig. 2a. Thus from Eq. 5 to Eq. 7 the concentration of reticulocytes ($C_{RET}(t)$) and RBCs ($C_{RBC}(t)$) are given by:

$$C_{RET}(t) = \frac{N_{RET}(t)}{V(t)} \tag{21}$$

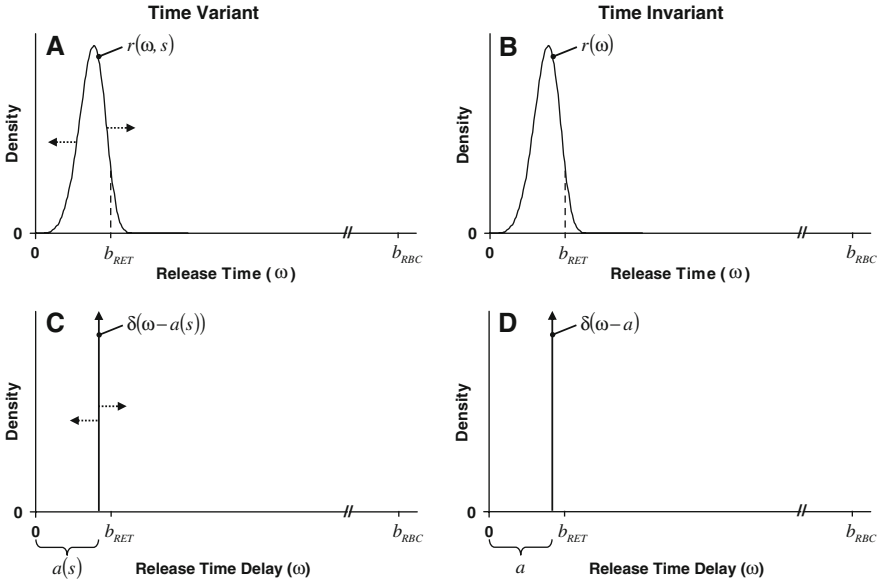

Fig. 2 Schematic of the differences between the time variant distribution (**a**), time invariant distribution (**b**), time variant "point distribution" (**c**), and time invariant "point distribution" (**d**) cellular lifespan models. Time variance is illustrated by horizontal dotted arrows. Also illustrated in each panel is the relationship between each of the release time delay "distributions", the time from stimulation of an erythroid precursor cell to transformation of the subsequently stimulated reticulocyte into a mature RBC (b_{RET}), and the time from stimulation of a erythroid precursor cell to senescence/destruction of the subsequently stimulated RBC (b_{RBC}). The stimulation time is denoted by s

$$C_{RBC}(t) = \frac{N_{RBC}(t)}{V(t)} \tag{22}$$

where $V(t)$ is given by Eq. 15. The parameter for the time from stimulation of a erythroid precursor cell to senescence/destruction of the subsequently stimulated RBC, b_{RBC}, was fixed to '$E\{\Omega\}$ + RBC lifespan', where $E\{\cdot\}$ denotes the mathematical expectation of a random variable and in this instance is the expectation taken with respect to the initial steady-state release time delay distribution (i.e., $r(\omega, t_0)$). The normal RBC lifespan has previously been determined in sheep using [^{14}C] cyanate label and found to be 114 days [29].

The reticulocyte and RBC-plasma EPO concentration relationship, accounting for subject growth, was modeled by simultaneously fitting Eqs. 21 and 22 (along with supporting Eqs. 13–15 and Eqs. 18–20) using the fitted plasma EPO concentration and animal mass, the observed reticulocyte count, and the observed RBC count concentration-time data of each subject.

Comparison to other lifespan models

The formulated time variant cellular lifespan distribution model (Fig. 2a) was compared to the identical time invariant cellular lifespan distribution model, as well as the time variant and time invariant "point distribution" cellular lifespan models. Each model was fit to data from each animal. Replacement of $r(\omega, u)$ in Eq. 19 with $r(\omega)$ gives the following identical *time invariant* cellular lifespan distribution model:

$$r(\omega) = \begin{cases} \frac{k}{\lambda} \cdot \left[\frac{\omega - \theta}{\lambda}\right]^{k-1} \cdot exp\left(-\left[\frac{\omega - \theta}{\lambda}\right]^{k}\right) & \text{for } \omega \geq \theta \text{ and } 0 \leq \omega < \infty \\ 0 & \text{otherwise} \end{cases} \tag{23}$$

where θ is the time invariant location parameter of the Weibull distribution (Fig. 2b). In the time invariant cellular lifespan distribution model the distribution of release time delays (and lifespans) is constant and independent of the time of stimulation. Models of time invariant distributions of cellular lifepsans have previously been described in detail [22].

The *time variant* "point distribution" cellular lifespan model (Fig. 2c), is obtained by replacing in Eq. 19 the time variant Weibull distribution (i.e., $r(\omega, u)$ given by Eq. 17) with a time variant dirac delta function, $\delta(\omega - a(u))$, which upon simplification gives:

$$N(t) = \int_{t-b}^{x(t)} f_{stim}(u)\,du - U(t - T_{P1}) \cdot [1 - F_1] \cdot \int_{min(x(T_{P1}),t-b)}^{x(T_{P1})} f_{stim}(u)\,du$$
$$- U(t - T_{P2}) \cdot [1 - F_2] \cdot \int_{min(x(T_{P2}),t-b)}^{x(T_{P2})} f_{stim}(u)\,du$$

$$+U\left(t-T_{P2}\right)\cdot\left[1-F_2\right]\cdot\left[1-F_1\right]\cdot\int_{min(x(T_{P1}),t-b)}^{x(T_{P1})}f_{stim}\left(u\right)du \tag{24}$$

with:

$$\begin{aligned}x\left(t\right)&=t-a\left(x\left(t\right)\right)\\ a'\left(s\right)&>-1\\ b_{RET}>a\left(s\right)&\geq 0\end{aligned}$$

where $x\left(t\right)$ is the time of stimulation of cells currently entering the sampling compartment and $a\left(s\right)$ is the time variant "point" cellular release time delay given by the end constrained quadratic spline function of the same form as that used for $\theta\left(s\right)$ (Appendix F). The constraint that $a'\left(s\right)>-1$ is needed to ensure a unique solution to $x\left(t\right)$ as previously discussed [23]. Additionally, $a\left(s\right)$ is constrained to be less than b_{RET} because if $a\left(s\right)\geq b_{RET}$ then no reticulocytes would be present in the sampling compartment (at least for some period of time), which was never observed. For the time variant "point distribution" model all cells stimulated at a given stimulation time have the same release time delay and lifespan, the latter which is defined by $b-a\left(s\right)$. However, cells stimulated at different times may have different release time delays and lifespans. The time variant and time invariant "point distribution" cellular lifespan model and the $x\left(t\right)$ function have previously been presented [23].

The *time invariant* "point distribution" cellular lifespan model, is obtained by replacing in Eq. 19 the time variant Weibull distribution with a time invariant dirac delta function, $\delta\left(\omega-a\right)$, which upon simplification gives:

$$\begin{aligned}N\left(t\right)=&\int_{t-b}^{t-a}f_{stim}\left(u\right)du-U\left(t-T_{P1}\right)\cdot\left[1-F_1\right]\cdot\int_{min(T_{P1}-a,t-b)}^{T_{P1}-a}f_{stim}\left(u\right)du\\ &-U\left(t-T_{P2}\right)\cdot\left[1-F_2\right]\cdot\int_{min(T_{P2}-a,t-b)}^{T_{P2}-a}f_{stim}\left(u\right)du\\ &+U\left(t-T_{P2}\right)\cdot\left[1-F_2\right]\cdot\left[1-F_1\right]\cdot\int_{min(T_{P1}-a,t-b)}^{T_{P1}-a}f_{stim}\left(u\right)du\end{aligned} \tag{25}$$

where:

$$b_{RET}>a\geq 0$$

and a is the time invariant "point" cellular release time delay (Fig. 2d). In the time invariant "point distribution" cellular lifespan model all cells have the identical release

time delay and lifespan (i.e., resulting in a constant value for the lifespan, $b-a$), irregardless of the time of stimulation. The relationship between the time variant and time invariant "point distribution" cellular lifespan models can be also be observed by replacement of $a\,(s)$ in Eq. 24 with the constant a, which upon simplification will give Eq. 25.

The differences between the four cellular lifespan models are illustrated in Fig. 2. The objective function value, Akaike's Information Criterion (AIC) value [30], and the squared correlation coefficient (R^2) of the observed vs. predicted concentrations (across all animals) were used as goodness-of-fit criteria to compare the four different cellular lifespan models. Additionally, the means and standard deviations of the common parameters of the four different models were compared.

Computational details

All modeling was conducted using WINFUNFIT, a Windows (Microsoft) version evolved from the general nonlinear regression program FUNFIT [31], using weighted least squares. Motivated by the enumeration of the cellular data (i.e., a Poisson process) and the large differences in scale of the reticulocyte and RBC data, data points were weighted by y_{obs}^{-1}, where y_{obs} is the observed reticulocyte or RBC concentration. The fitted models required the numerical solution to a one-dimensional integral (Eqs. 19, 24, and 25). This was done by using the FORTRAN 90 subroutine QDAGS from the IMSL® Math Library (Version 3.0, Visual Numerics Inc., Houston, TX). QDAGS is a univariate quadrature adaptive general-purpose integrator that is an implementation of the routine QAGS [32]. The relative error for the QDAGS routine was set at 0.1% for all numerical integrations. Additionally, the implicit function $x\,(t)$ had to be solved to determine the upper integration bound of Eq. 24, which was done using the FORTRAN 90 subroutine ZREAL from the IMSL® Math Library. ZREAL is a nonlinear equation solver that finds the zero of a real function using Müller's method. The relative error for the ZREAL routine was set at 0.01%.

To summarize the uncertainty in the individual subject parameter estimates for the time variant lifespan distribution model, the mean percent standard error (MSE%) of the estimate was calculated for each parameter as:

$$\mathrm{MSE\%} = \frac{1}{n} \cdot \sum_{i=1}^{n} \frac{\mathrm{SE}_i}{|\mathrm{P}_i|} \cdot 100 \tag{26}$$

where SE_i and P_i are the standard error of the parameter and the estimate of the parameter for the ith subject, respectively, and n is the number of subjects. The mean lifespan of circulating reticulocytes at the current stimulation time was determined over time for each subject by analytically calculating the mathematical expectation of the circulating lifespan, conditional on s (i.e., $E\,\{\mathrm{T}|s\}$), with the expectation taken with respect to the distribution given by Eq. 12, where $r\,(\cdot, s)$ is the fitted Weibull distribution (Appendix G).

Statistical analysis

For the time variant lifespan distribution model, the minimum, maximum, and study end mean circulating reticulocyte lifespans at the current stimulation time were statistically compared to the mean initial (t_0) or baseline lifespan (denoted by $\mu_{RET,0}$) with paired two tailed Student's t-tests using Microsoft® Excel 2002 SP3 (Microsoft Corporation, Redmond, WA). Statistically significant differences were determined at the $\alpha = 0.05$ type I experimentwise error rate. To control the experimentwise error rate inflation due to multiple comparisons, a stepdown Bonferroni method was used to adjust the *P-values* from the paired t-tests [33].

Results

The profiles and the simultaneous fit to the plasma EPO, reticulocyte, and RBC concentration data for two representative animals (Panels A and B) is displayed in Fig. 3 for the time variant cellular lifespan distribution model. The dynamic relationship between the phlebotomy induced anemia, plasma EPO, reticulocyte, and RBC concentrations was modeled. The plasma EPO concentrations rapidly rose within hours of both phlebotomies, and then returned to baseline concentrations approximately 5 days post-phlebotomy. The reticulocyte concentrations began to increase 1–2 days following the rise in plasma EPO concentrations, peaking several days later, while the RBC concentrations steadily rose following both phlebotomies. The formulated time variant cellular lifespan distribution model also fit the data very well across a wide range of concentrations. The R^2 of observed vs. predicted reticulocyte concentrations was 0.952 and observed vs. predicted RBC concentrations was 0.964 across all animals.

The PD parameters of the time variant lifespan distribution model are summarized in Table 1. In general, the parameters of the model were well estimated with MSE% of less than 20% for all parameters, with many less than 5%. Not surprisingly, the scale (λ) and shape (k) parameters of the release time delay p.d.f. were not as well estimated and had higher MSE%. A relatively high amount of subject to subject variability was observed in the E_{max} and EC_{50} parameters of the transduction function, with means of 4.97×10^{10} cells/kg/day and 66.6 mU/ml, respectively. The weight normalized total blood volume was estimated at 81.0 (2.38) (mean (SD)) ml/kg or 8.10%, consistent with the standard blood volume estimates in mammals of 6–11% of body weight [12], and slightly higher than means previously determined in sheep ranging from 57.6 to 74.4 ml/kg (34). The incorporation of blood volume expansion due to animal growth was an important consideration of the model, as animals grew on average 4.1 kg or 17% of their initial body weights over the course of the experiments. The average initial (t_0) body weight and rate constant of growth were estimated at 22.3 (2.31) kg and 0.00379 (0.00385) 1/day, respectively. The monoexponential fit to body weight data from the presented two representative subjects is displayed in Fig. 3 (inset). While the monoexponential function (Eq. 16) does not fit the observed animal weight data exactly, it is used to represent the lean body mass that will be more representative of changes in erythropoietic progenitor cell mass and blood volume, since these will not likely change substantially with transient increases and losses of adipose that may be

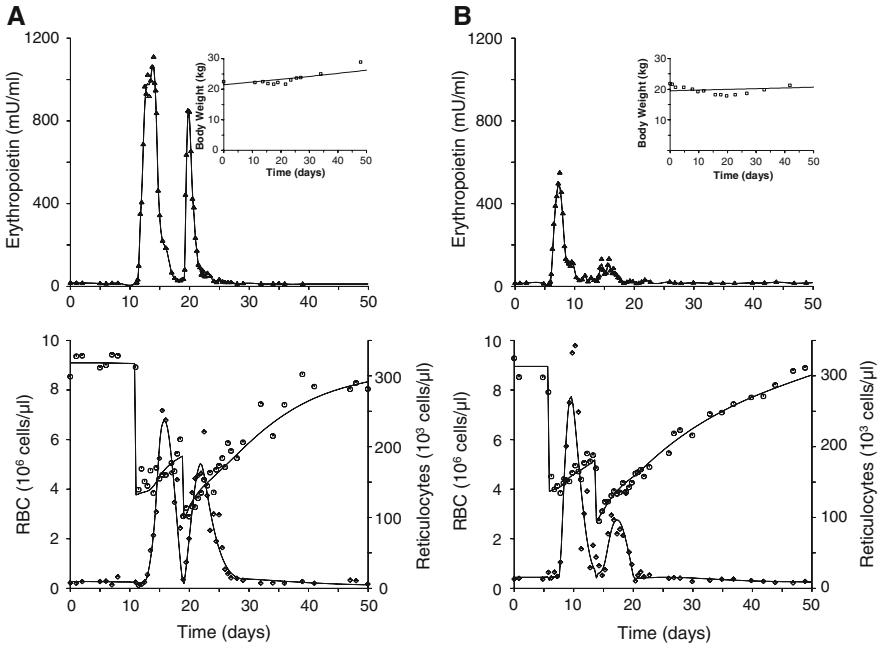

Fig. 3 Representative individual subject fits (curves) of the time variant lifespan distribution model to observed plasma EPO ( ) concentrations, reticulocyte ( ) concentrations, RBC ( ) concentrations, and body weight (□) (inset). (**a**) and (**b**) are different subjects

Table 1 Parameter estimates for the reticulocyte and RBC time variant lifespan (release time delay) distribution model ($n = 4$)

	E_{max} (10^{10} cells/kg/day)	EC_{50} (mU/ml)	k_{bio} (1/day)	V_n (ml/kg)	θ_0 (day)	λ	k	b_{RET} (day)	$\mu^{a}_{RET,0}$ (day)
Mean	4.97	66.6	0.126	81.0	1.28	1.09	1.55	1.99	0.304
SD	2.08	35.4	0.0271	3.28	0.343	0.476	0.285	0.518	0.0862
MSE%	0.5%	0.7%	11.2%	1.0%	4.4%	10.7%	17.2%	2.6%	N/A

[a] Secondary parameter
SD: Standard deviation
MSE%: Mean percent standard error (Eq. 26)
N/A: Not applicable

represented in the observed body weight. Furthermore, an exponential model was utilized for the body weight instead of a linear model to prevent the possibility of negative animal body weight prior to time t_0. From the number of measured cells removed by each phlebotomy and the model estimated number of cells in the circulation immediately prior to each phlebotomy the fraction of cells remaining following the first and second phlebotomies (F_1 and F_2, respectively) were estimated at 0.409 (0.0721) and 0.571 (0.0963), respectively. The baseline minimum release time delay between stimulation in the bone marrow and the subsequent release of the stimulated

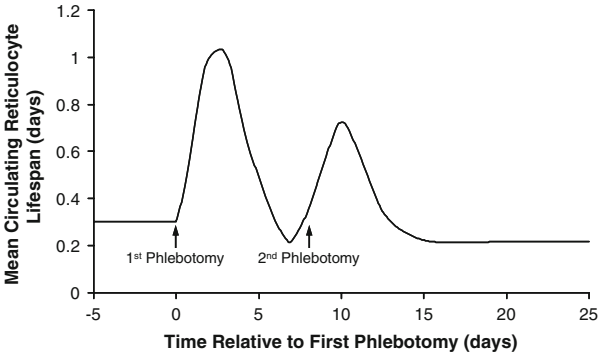

Fig. 4 Average mean circulating reticulocyte lifespan for the time variant lifespan distribution model calculated according to Appendix G from the parameter and $\theta\,(t)$ estimates for each individual subject ($n = 4$)

erythrocyte(s) into the systemic circulation (θ_0) was estimated at 1.28 (0.343) days, while the mean baseline release time delay of an erythrocyte was 2.26 (0.729) days with a constant (i.e., time invariant) standard deviation of 0.659 (0.289) days. Finally, the time between stimulation in the bone marrow and maturation of the erythrocyte from a reticulocyte to a mature RBC (b_{RET}) was estimated at 1.99 (0.518) days.

The average mean circulating reticulocyte lifespan at the current stimulation time is displayed in Fig. 4. From the baseline value of 0.304 days ($\mu_{RET,0}$, Table 1) it rapidly increased over 3-fold following the first phlebotomy to a value of 1.03 days ($P = 0.009$). Following the initial peak, the mean circulating reticulocyte lifespan dropped down to near baseline values before rising again after the second phlebotomy. Following the second reticulocyte lifespan peak, the study end mean lifespan dropped to a value of 0.218 days, similar to the baseline value ($P > 0.05$). The minimum mean circulating reticulocyte lifespan was also not significantly different from the baseline lifespan ($P > 0.05$), nor was the minimum lifespan between the two phlebotomies significantly different from $\mu_{RET,0}$ ($P > 0.05$). The average percentage of erythrocytes at baseline (i.e., at day 0) being released as reticulocytes was estimated at 43.0% (57.0% released as mature RBCs), while the average maximal proportion of stimulated cells to be released as reticulocytes was estimated at 89.5%, with only 10.5% of stimulated cells released as mature RBCs. The two-fold increase in the percentage of erythrocytes being released as reticulocytes (and nearly six-fold decrease in the percentage released as mature RBCs) illustrates the dramatic changes that occur in both the release time delay distribution and the type of erythrocytes being released under stress erythropoietic conditions in sheep.

The comparison of the time variant distribution, the time invariant distribution, the time variant "point distribution", and time invariant "point distribution" of cellular lifespan models is summarized in Table 2. A schematic of the model differences is displayed in Fig. 2. In general, all models fit the RBC data equally well, with R^2 values near 0.96, however, the time invariant models fit the reticulocyte data poorly with R^2 values near 0.46. The mean objective function value was the smallest for the time variant lifespan distribution model. However, in three of the four animals the time

Table 2 Comparison of goodness-of-fit criteria and common parameter estimates of four different cellular lifespan models ($n = 4$). Only a single R^2 value was determined across all animals. Other values represented as mean (standard deviation)

Model	Time variant distribution	Time invariant distribution	Time variant "point distribution"	Time invariant "point distribution"
No. of fitted parameters	21	8	19	6
R^2 reticulocytes	0.952	0.455	0.942	0.470
R^2 RBCs	0.964	0.966	0.964	0.962
Objective function	62,300 (37,300)	152,000 (73,100)	63,100 (35,100)	157,000 (73,100)
AIC	629 (98.4)	685 (91.9)	627 (93.8)	684 (86.8)
E_{max} (10^{10} cells/kg/day)	4.97 (2.08)	5.36 (2.00)	5.43 (2.44)	5.65 (2.67)
EC_{50} (mU/ml)	66.6 (35.4)	71.0 (32.0)	71.7 (41.0)	77.5 (47.1)
k_{bio} (1/day)	0.126 (0.0271)	0.146 (0.0680)	0.119 (0.0276)	0.137 (0.0595)
V_n (ml/kg)	81.0 (3.28)	82.9 (4.85)	83.5 (3.48)	81.9 (4.83)
b_{RET} (day)	1.99 (0.518)	1.76 (0.047)	1.90 (0.289)	1.28 (0.127)
$\mu_{RET,0}$[a] (day)	0.304 (0.0862)	0.403 (0.162)	0.123 (0.0487)	0.135 (0.049)
$\mu_{RET,MAX}$[a] (day)	1.12 (0.238)	N/A	1.02 (0.198)	N/A

[a] Secondary parameter
N/A: Not applicable

variant "point distribution" was preferred over the other models based on the AIC. In the remaining animal the AIC was the lowest for the time variant distribution model. On average, AIC was the smallest for the time variant "point distribution" model. The stimulation function parameters (i.e., E_{max}, EC_{50}, and k_{bio}) and the weight normalized total blood volume were very similar across all models indicating a good model robustness for estimation of these parameters among the models. The mean b_{RET} was similar among most of the models, except for the time invariant "point distribution" cellular lifespan model. The baseline circulating reticulocyte lifespan ($\mu_{RET,0}$) was approximately 3-fold lower in the "point distribution" models than in the distribution models. For the time variant lifespan models the mean maximal circulating reticulocyte lifespans ($\mu_{RET,MAX}$) in each animal were similar, however, the increase from baseline was nearly 10-fold for the "point distribution" model.

Discussion

Two basic parameterizations of a time variant cellular lifespan distribution PD model were formulated to account for changes over time in the underlying lifespan p.d.f. of cellular populations. The presented model extends recent cellular lifespan models that assumed a single (i.e., a "point distribution") *time variant* cellular lifespan [23] and models that assumed a *time invariant* distribution of cellular lifespans [22]. Two important assumptions of the proposed PD model are: (1) the stochastic independence

of cells, and (2) that following production/stimulation subsequent changes in the environment do not alter the cellular disposition. The effects of subject growth on production or stimulation rate and on sampling space volume were also incorporated into the model. Additionally, the time variance of the underlying lifespan distribution can readily be incorporated into any of the parameters of the lifespan p.d.f., as either a non-parametric function of time or if more is known about the biological system, a function of the cellular production environment. By choosing a flexible arbitrary p.d.f. with a corresponding cumulative density function (c.d.f.) that can be analytically or otherwise rapidly evaluated, the proposed PD model can be fit to observed cellular concentration data requiring only a suitable numerical one dimensional integration solver. Furthermore, the production or stimulation rate in the model can be any analytical function that depends on endogenous growth factors and/or exogenous drugs.

A single time variant release time delay p.d.f. was utilized in the fitted equations for both the reticulocytes and RBCs (Eq. 19), with a fixed time, b_{RET}, from stimulation of an erythropoietic cell to transformation from a reticulocytes (an immature RBC) into a mature RBC (Fig. 2a). The presented model allows for a fraction of the red cells to be released directly into the systemic circulation as mature RBCs, as cells with release time delays $\geq b_{RET}$ are released into the sampling compartment as mature erythrocytes. The ability to account for the release of mature RBCs is particularly important when dealing with ruminants, such as sheep, that under basal, non-erythropoietically stimulated conditions release the majority of their red cells into the systemic circulation directly from the bone marrow as mature RBCs [8], and thus partially explaining the very low basal reticulocyte percentage in ruminants (0.1–0.2%) [12]. While a common release time delay p.d.f. is justified on a physiological basis, a fixed time of development from stimulation of progenitor cells to development into a mature RBC is a simplification of the underlying physiology. However, the utilized time variant cellular lifespan distribution model was chosen based on the knowledge that: less developmentally mature and hence younger reticulocytes (RBCs) are released under stress erythropoiesis [7,9–11], and that under basal, non-erythropoietically stimulated conditions sheep release the majority of their red cells directly from the bone marrow as mature RBCs [8]. Thus, the model captures the primary kinetic features of the immature RBC physiology, which would not be possible using a direct parameterization of a time variant reticulocyte lifespan (i.e., as given by Eq. 3).

The distribution of circulating reticulocyte lifespans at the current stimulation time can be determined from Eq. 12, and subsequently the mean circulating reticulocyte lifespan was calculated (Appendix G), as displayed in Fig. 4. Similar to previous results with a single phlebotomy and a "point distribution" of circulating reticulocyte lifespans (residence times) [23], the mean circulating reticulocyte lifespan rapidly increased approximately 3-fold shortly after the first phlebotomy ($P = 0.009$). However, unlike previous results, the mean reticulocyte lifespan did not drop significantly below the baseline lifespan following either phlebotomy ($P > 0.05$). The difference may be attributed to the small sample sizes in both studies ($n = 5$ and $n = 4$, respectively), accounting for subject growth in the present analysis, and/or the incorporation of a distribution of lifespans instead of a single lifespan, among other factors. The circulating reticulocyte lifespan in Fig. 4 begins to increase prior to the 2nd phlebotomy, which

may be the same but somewhat muted rebound phenomenon previously observed following a single acute phlebotomy [23]. The estimated approximately 3-fold increase in the circulating reticulocyte lifespan in both sheep studies is consistent with estimates in humans of a 2- to 3-fold increase following stress erythropoiesis [35] and with the exogenous administration of erythropoietin [20].

The time variant cellular lifespan distribution model represents the most general case and the other three models are simplified "special cases" of this model. The comparison of the four cellular lifespan models (Fig. 2) indicates that the time variant models were preferred to the time invariant models based on the objective function, R^2, and AIC values (Table 2). The two time variant cellular lifespan models resulted in similar fits, with the time variant "point distribution" model resulting in a lower AIC in three of the four animals. Hence, in the majority of cases the more complicated time variant distribution cellular lifespan model was not preferred to the time variant "point distribution" cellular lifespan model. These results comparing the distribution and the "point distribution" cellular lifespan models are consistent with results obtained by other investigators comparing a time invariant distribution cellular lifespan model to a time invariant "point distribution" cellular lifespan model [22]. However, the time variant "point distribution" model resulted in a very short estimate of the baseline circulating reticulocyte lifespan of 0.123 (0.0487) days and a maximal increase in the circulating reticulocyte lifespan of nearly 10-fold, which is inconsistent with estimated increases in circulating reticulocyte lifespan in humans of 2- to 3-fold following stress erythropoiesis [20,35]. The most likely reason for the apparent physiologically unrealistic estimates of these values is that the "point distribution" of cellular release time delays for this model (Fig. 2c) requires that all erythrocytes released from the bone marrow into the systemic circulation be released as reticulocytes. While the model could be extended to allow for all erythrocytes to be released from the bone marrow as either reticulocytes or mature RBCs depending on the stimulation time, this would cause the fitted reticulocyte concentration to drop to zero when $a(s) \geq b_{RET}$, which was never observed. The constraint on the type of erythrocyte released into the systemic circulation given by the time variant "point distribution" cellular lifespan model is in contrast to the more general nature of the time variant distribution model (Fig. 2a). With the distribution model, erythrocytes with a release time delay (i.e., ω) less than b_{RET} enter the systemic circulation as a reticulocyte while erythrocytes with an $\omega \geq b_{RET}$ enter the circulation as a mature RBC, consistent with the known physiology in sheep where a fraction of the erythrocytes enter the circulation as a mature RBC [8,12]. Thus the underlying physiology must be considered when selecting the most appropriate cellular lifespan model, and not just the goodness-of-fit criteria (e.g., AIC).

The addition of a distribution of release time delays to the time variant lifespan model over a time variant single "point distribution" lifespan [23] offers modeling cellular responses in a more physiologically realistic manner. The described model allowed for the estimation of the proportion of the erythrocytes being released directly into the systemic circulation from the bone marrow as mature RBCs. Apparently, estimates of the proportion of erythrocytes released as reticulocytes or RBCs have not been previously determined in sheep. Other potential applications of the presented model are to account for changes in RBC lifespan that are due to production

under stress erythropoiesis conditions, as previously demonstrated in some animal models [4,36,37]. Even though not accounted for in the model, a reduced RBC lifespan due to stress erythropoiesis stimulation conditions was not a concern because the lifespan would have to be reduced to less than 50 days to have an effect on the modeling, since this was the longest time period of observation following the first phlebotomy.

In addition to the stochastic independence assumption of cells, the other key assumption of the model is that the disposition of cells *following* production or stimulation is not affected by changes in the environmental conditions. Apparently, all PD models of cellular response presented to date either implicitly utilize this assumption [14,20–23,38], or assume that cellular age has no affect on the probability of cellular death/transformation (i.e., a cell "pool" or "random hit lifespan" model) [13,39,40]. The lack of a "environmental effect" assumption may not be reasonable if the environmental conditions that a cell is exposed to over its lifetime vary substantially over time, particularly for cells with relatively long lifespan (relative to the rate of change in the environmental conditions). For circulating reticulocytes, which have a relatively short lifespan, there is evidence in rats that the RNA content (and hence age) of cells depends on the conditions under which the reticulocytes developed [41]. Similar conclusions have been obtained in humans, that under normal conditions the properties of the erythrocyte lifespan are determined by the conditions under which they are formed [4]. Thus for reticulocytes their disposition may well be determined at the time of stimulation. However, if changes in the environmental conditions (e.g., plasma EPO concentrations) *following* production or stimulation of reticulocytes (or mature RBCs) do substantially affect their circulating lifespan this key assumption of the current model would be violated. Hence, extensions of the presented model to incorporate the effects of changing environmental conditions on the disposition of the cells are still needed, particularly under pathological disease conditions. Further work in this area is in progress.

Conclusion

In summary, a time variant cellular lifespan distribution PD model was formulated to account for changes over time in the underlying lifespan probability density function of cellular populations. The model extends recent cellular lifespan models that assumed a single (i.e., a "point distribution") *time variant* cellular lifespan and models that assumed a *time invariant* distribution of cellular lifespans. Furthermore, the model developed in the present study was used to determine the time variant circulating reticulocyte lifespan in sheep following stress erythropoiesis conditions. The proportion of erythrocytes released from the bone marrow as reticulocytes was estimated by the model to increase over 2-fold following phlebotomy. The time variant cellular lifespan distribution model was compared to three simpler cellular lifespan models derived as specific cases of the proposed time variant lifespan model. These comparisons indicated the importance of accounting for a time variant cellular lifespan for reticulocytes stimulated under stress erythropoiesis conditions. Additionally, they indicated that the selection of the most appropriate model should not solely be based on conventional

goodness-of-fit metrics but must also consider the underlying cellular physiology. The presented PD model readily allows incorporation of time variant lifespan distributions when considering populations of cells whose production or stimulation depends on endogenous growth factors and/or exogenous drugs.

Acknowledgements The recombinant human EPO used in the EPO RIA was a gift from Dr. H. Kinoshita of Chugai Pharmaceutical Company, Ltd. (Tokyo, Japan). The rabbit EPO antiserum used in the EPO RIA was a generous gift from Gisela K. Clemens, PhD. This work was supported in part by the United States Public Health Service, National Institute of Health Program Project Grant 2 P01 HL046925-11A1 and R21 GM57367.

Appendices

Appendix A. Derivation of Eq.6

To account for the removal by phlebotomy of a certain fraction, $1 - F$, of cells at time $t = T_P$ is equivalent to label this fraction of cells at time T_P and only counting the unlabeled cells.

$$N_{tot}(t) = N_{lab}(t) + N_{unlab}(t) \tag{A1}$$

where: $N_{tot}(t) \equiv$ total number of cells, $N_{lab}(t) \equiv$ number of labeled cells, and $N_{unlab}(t) \equiv$ number of unlabeled cells.

The interest is to quantify the number of unlabeled cells (i.e., the cells not removed by the phlebotomy), which from Eq. A1 is given by:

$$N(t) \equiv N_{unlab}(t) = N_{tot}(t) - N_{lab}(t) \tag{A2}$$

If it is assumed that the cells behave independent of each other regardless of being labeled or not (which is a basic assumption of the derivation), then the superposition principle holds. Let the probability that a cell that enters the sampling space at time z is still present at time $z + x$, where x is a non-negative time value, be denoted by $P(x, z)$, then according to the superposition principle that arises from a linear cellular disposition:

$$N_{tot}(t) = \int_{-\infty}^{t} f_{prod}(u) \cdot P(t - u, u)\, du \tag{A3}$$

Equation A3 can be written as:

$$N_{tot}(t) = \int_{-\infty}^{t} f_{prod}(u) \cdot P(t-u,u)\,du$$
$$= \int_{-\infty}^{min(t,T_p)} f_{prod}(u) \cdot P(t-u,u)\,du$$
$$+ \int_{min(t,T_p)}^{t} f_{prod}(u) \cdot P(t-u,u)\,du \quad \text{(A4)}$$

where $min\left(t, T_p\right)$ is the minimum value of t and T_p. If the production of cells ($f_{prod}(t)$), i.e., input of new cells into the sampling space, is stopped at time T_P then the second integral in Eq. A4 is equal to zero for $t > T_p$ since $f_{prod}(t) = 0$. Additionally, if $t \leq T_p$ the second integral is still equal to zero. Hence total number of cells would be:

$$N_{tot}(t) = \int_{-\infty}^{min(t,T_p)} f_{prod}(u) \cdot P(t-u,u)\,du \quad \text{(A5)}$$

Equation A5 is equivalent to labeling all cells in the sampling space at time T_P and counting the number of labeled cells thereafter. Thus, if only a fraction, $1 - F$, of the cells present at time T_P are labeled (i.e., removed by the phlebotomy) then the number of labeled cells is:

$$N_{lab}(t) = U(t - T_P) \cdot [1 - F] \cdot \int_{-\infty}^{T_p} f_{prod}(u) \cdot P(t-u,u)\,du \quad \text{(A6)}$$

where U is the unit step function described by:

$$U(\mathbf{x}) = \begin{cases} 1 & \text{if } x \geq 0 \\ 0 & \text{otherwise} \end{cases} \quad \text{(A7)}$$

which has been introduced in Eq. A6 to make thek equation valid for any value of t. Equations A2, A3, and A6 give:

$$N(t) = \int_{-\infty}^{t} f_{prod}(u) \cdot P(t-u,u)\,du - U(t - T_P)$$
$$\cdot [1 - F] \cdot \int_{-\infty}^{T_p} f_{prod}(u) \cdot P(t-u,u)\,du \quad \text{(A8)}$$

If $\ell(\tau, z)$ denotes the *time variant* p.d.f. of cellular lifespans, where τ is the cellular lifespan and z is an arbitrary time of production, then:

$$P(x, z) = 1 - \int_0^x \ell(\tau, z)\, d\tau \tag{A9}$$

which can be recognized as the unit response of Eq. 1. Inserting Eq. A9 into Eq. A8 gives:

$$N(t) = \int_{-\infty}^{t} f_{prod}(u) \cdot \left[1 - \left[\int_0^{t-u} \ell(\tau, u)\, d\tau\right]\right] du - U(t - T_P)$$
$$\cdot [1 - F] \cdot \int_{-\infty}^{T_p} f_{prod}(u) \cdot \left[1 - \left[\int_0^{t-u} \ell(\tau, u)\, d\tau\right]\right] du \tag{A10}$$

For $t \geq T_P \quad U(t - T_P) \equiv 1$ and Eq. A10 simplifies to the following expression:

$$N(t) = F \cdot \int_{-\infty}^{T_P} f_{prod}(u) \cdot \left[1 - \left[\int_0^{t-u} \ell(\tau, u)\, d\tau\right]\right] du$$
$$+ \int_{T_P}^{t} f_{prod}(u) \cdot \left[1 - \left[\int_0^{t-u} \ell(\tau, u)\, d\tau\right]\right] du, \quad t \geq T_P \tag{A11}$$

Completing the derivation of Eq. 6.

Appendix B. Derivation of Eq. 8

The probability that a cell is present in the sampling space is given by the intersection of two events: the time since stimulation is less than b (Event 1) and the cell has been released into the sampling space (Event 2). The probabilities of these two individual events are given by:

$$P(\text{Event1}) = P(t - s < b) = 1\{t - s < b\} = 1 - U(t - s - b) \tag{B1}$$

$$P(\text{Event 2}) = P(\Omega \leq t, s) = \int_0^{t-s} r(\omega, s)\, d\omega, \quad t \geq s, \quad 0 \leq \omega < \infty \tag{B2}$$

Due to the independence assumption of the two events, the probability of both events occurring (i.e., the intersection of the events) is simply the product of the individual event probabilities, as given by:

$$P\,(\text{Event } 1 \cap \text{Event } 2) = P\,(\text{Event1}) \cdot P\,(\text{Event } 2) = [1 - U\,(t - s - b)] \cdot \int_0^{t-s} r\,(\omega, s)\,d\omega, t \geq s, \quad 0 \leq \omega < \infty \tag{B3}$$

Given the assumed independent disposition of cells following stimulation, the probability that a cell is present in the sampling space is the unit response of the cell, completing the derivation of Eq. 8.

Appendix C. Derivation of Eq.11

Following the derivation of Eq. 6 (Appendix A), from Eq. A2 the interest is to quantify the number of unlabeled cells (i.e., the cells not removed by the phlebotomy). Let the probability that the time since stimulation, x, for a cell is less than some positive constant b (i.e., probability of Event 1) be denoted by $P_1\,(x)$. Equivalently, $P_1\,(x)$ can be thought of as the probability that a cell exists as the cell type of interest (either outside or in the sampling space). Additionally, let the probability that a cell stimulated at time s has been released into the sampling space at time $s + x$, be denoted by $P_2\,(x, s)$ (i.e., probability of Event 2). If these two events are assumed to be independent (as is assumed in the model formulation, see Appendix B), then the probability that a cell is present in the sampling space as the cell type of interest (i.e., the intersection of Event 1 and Event 2) is given by the multiplication of these probabilities. Then according to the superposition principle that arises from a linear cellular disposition:

$$N_{tot}\,(t) = \int_{-\infty}^{t} f_{stim}\,(u) \cdot P_1\,(t - u) \cdot P_2\,(t - u, u)\,du \tag{C1}$$

which can also be written as:

$$\begin{aligned} N_{tot}\,(t) &= \int_{-\infty}^{t} f_{stim}\,(u) \cdot P_1\,(t - u) \cdot P_2\,(t - u, u)\,du \\ &= \int_{-\infty}^{min(t,T_P)} f_{stim}\,(u) \cdot P_1\,(t - u) \cdot P_2\,(t - u, u)\,du \\ &\quad + \int_{min(t,T_P)}^{t} f_{stim}\,(u) \cdot P_1\,(t - u) \cdot P_2\,(t - u, u)\,du \\ &= \int_{-\infty}^{min(t,T_P)} f_{stim}\,(u) \cdot P_1\,(t - u) \end{aligned}$$

$$
\begin{aligned}
&\cdot \left[P_2\left(min\left(t, T_P\right) - u, u\right) + P_2\left(t - u, u\right) - P_2\left(min\left(t, T_P\right) - u, u\right)\right] du \\
&+ \int_{min(t,T_P)}^{t} f_{stim}\left(u\right) \cdot P_1\left(t - u\right) \cdot P_2\left(t - u, u\right) du \\
= &\int_{-\infty}^{min(t,T_P)} f_{stim}\left(u\right) \cdot P_1\left(t - u\right) \cdot P_2\left(min\left(t, T_P\right) - u, u\right) du \\
&+ \int_{-\infty}^{min(t,T_P)} f_{stim}\left(u\right) \cdot P_1\left(t - u\right) \\
&\cdot \left[P_2\left(t - u, u\right) - P_2\left(min\left(t, T_P\right) - u, u\right)\right] du \\
&+ \int_{min(t,T_P)}^{t} f_{stim}\left(u\right) \cdot P_1\left(t - u\right) \cdot P_2\left(t - u, u\right) du
\end{aligned}
\tag{C2}
$$

where $min\left(t, T_P\right)$ is the minimum value of t and T_P. If the input of new cells into the sampling space were to be stopped at time T_P, then $f_{stim}\left(t\right)$ must be equal to zero when $t \geq T_P$ giving:

$$
\begin{aligned}
N_{tot}\left(t\right) = &\int_{-\infty}^{min(t,T_P)} f_{stim}\left(u\right) \cdot P_1\left(t - u\right) \cdot P_2\left(min\left(t, T_P\right) - u, u\right) du \\
&+ \int_{-\infty}^{min(t,T_P)} f_{stim}\left(u\right) \cdot P_1\left(t-u\right) \cdot \left[P_2\left(t-u, u\right) - P_2\left(min\left(t, T_P\right) - u, u\right)\right] du \\
&+ \int_{min(t,T_P)}^{t} 0 \cdot P_1\left(t - u\right) \cdot P_2\left(t - u, u\right) du \\
= &\int_{-\infty}^{min(t,T_P)} f_{stim}\left(u\right) \cdot P_1\left(t - u\right) \cdot P_2\left(min\left(t, T_P\right) - u, u\right) du \\
&+ \int_{-\infty}^{min(t,T_P)} f_{stim}\left(u\right) \cdot P_1\left(t-u\right) \cdot \left[P_2\left(t-u, u\right) - P_2\left(min\left(t, T_P\right) - u, u\right)\right] du
\end{aligned}
\tag{C3}
$$

Likewise, if $t < T_P$ then the integral of the third integrand of Eq. C2 would also be equal to zero, hence Eq. C3 is true for all t. Furthermore, when $t > T_P$ it is recognized that $P_2\left(t - s, s\right) - P_2\left(min\left(t, T_P\right) - s, s\right)$ is the probability that a cell stimulated at time s is released into the sampling space between time T_P and time t (if $t \leq T_P$ it's the probability of release between time t and time t, which is equal to zero). However, since

the input of new cells stopped at time T_P, then $P_2\,(t-s,s)-P_2\,(min\,(t,T_P)-s,s)$ must also be equal to zero giving:

$$\begin{aligned} N_{tot}\,(t) &= \int_{-\infty}^{min(t,T_P)} f_{stim}\,(u)\cdot P_1\,(t-u)\cdot P_2\,(min\,(t,T_P)-u,u)\,du \\ &\quad + \int_{-\infty}^{min(t,T_P)} f_{stim}\,(u)\cdot P_1\,(t-u)\cdot [0]\,du \\ &= \int_{-\infty}^{min(t,T_P)} f_{stim}\,(u)\cdot P_1\,(t-u)\cdot P_2\,(min\,(t,T_P)-u,u)\,du \end{aligned} \tag{C4}$$

Equation C4 is equivalent to labeling all cells in the sampling space at time T_P and counting the number of labeled cells. Thus if only a fraction, $1-F$, of the cells present at time T_P are labeled (i.e., removed by the phlebotomy) then the number of labeled cells is:

$$N_{lab}\,(t) = U\,(t-T_P)\cdot[1-F]\cdot\int_{-\infty}^{T_P} f_{stim}\,(u)\cdot P_1\,(t-u)\cdot P_2\,(T_P-u,u)\,du \tag{C5}$$

Equations A2, C1, and C5 give:

$$\begin{aligned} N\,(t) &= \int_{-\infty}^{t} f_{stim}\,(u)\cdot P_1\,(t-u)\cdot P_2\,(t-u,u)\,du \\ &\quad -U\,(t-T_P)\cdot[1-F]\cdot\int_{-\infty}^{T_P} f_{stim}\,(u)\cdot P_1\,(t-u)\cdot P_2\,(T_P-u,u)\,du \end{aligned} \tag{C6}$$

The probability that x is less than some positive constant b (i.e., $P_1\,(x)$) is either 1 or 0, since x either is or is not less than b, respectively. Therefore:

$$P_1\,(x) = 1-U\,(x-b) \tag{C7}$$

which can be recognized as the probability of Event 1 of Eq. B1. If $r\,(\omega,s)$ is the *time variant* p.d.f of cellular release time delays, where ω is the cellular release time delay and s is an arbitrary time of stimulation, then:

$$P_2(x,s) = \int_0^x r(\omega,s)\,d\omega \tag{C8}$$

which can be recognized as the probability of Event 2 of Eq. B2. Substitution of Eq. C7 and Eq. C8 in Eq. C6 results in:

$$\begin{aligned} N(t) &= \int_{-\infty}^{t} f_{stim}(u)\cdot[1-U(t-u-b)] \\ &\quad\cdot\left[\int_0^{t-u} r(\omega,u)\,d\omega\right]du \\ &\quad -U(t-T_P)\cdot[1-F]\cdot\int_{-\infty}^{T_P} f_{stim}(u)\cdot[1-U(t-u-b)] \\ &\quad\cdot\left[\int_0^{T_P-u} r(\omega,u)\,d\omega\right]du \\ &= \int_{t-b}^{t} f_{stim}(u)\cdot\left[\int_0^{t-u} r(\omega,u)\,d\omega\right]du - U(t-T_P)\cdot[1-F]\cdot \\ &\quad \int_{min(T_P,t-b)}^{T_P} f_{stim}(u)\cdot\left[\int_0^{T_P-u} r(\omega,u)\,d\omega\right]du \end{aligned} \tag{C9}$$

The unit step functions of the integrands are eliminated in the simplification step of Eq. C9 since it is recognized that the integrand will have a value of 0 at all times when $u < t-b$. However, by eliminating the units step functions the lower bound of the first integral in the second term of Eq. C9 must then be constrained to be the $min(T_P, t-b)$ to maintain the integrals evaluation to zero at all values of $u < t-b$. For $t-b < T_P \le t$ Eq. C9 further simplifies to the following expression:

$$\begin{aligned} N(t) &= \int_{t-b}^{t} f_{stim}(u)\cdot\left[\int_0^{t-u} r(\omega,u)\,d\omega\right]du - [1-F]\cdot\int_{t-b}^{T_P} f_{stim}(u) \\ &\quad\cdot\left[\int_0^{T_P-u} r(\omega,u)\,d\omega\right]du, \quad t-b < T_P \le t \end{aligned} \tag{C10}$$

It can also be observed from Eq. C9 that if T_P is not contained in the time interval from $t - b$ to t, only the first term is non-zero, giving the solution identical to Eq. 10. This completes the derivation of Eq. 11.

Appendix D. Derivation of Eq. 12

The cellular lifespan for a particular cell type of interest, defined as the time period from release of a cell into the sampling space to the time the cell is removed (or transformed) from the sampling space, is given by:

$$\tau = b - \omega, \quad 0 \leq \tau < b \tag{D1}$$

where ω denotes the time delay from cellular stimulation to appearance or release of the subsequently stimulated cell(s). Therefore it follows that:

$$\ell(\tau, s) \propto r(b - \tau, s), \quad 0 \leq \tau < b \tag{D2}$$

The normalizing factor for Eq. D2 is the definite integral of the release time delay p.d.f. from 0 to b, giving:

$$\ell(\tau, s) = \frac{r(b - \tau, s)}{\int_0^b r(\omega, s)\, d\omega}, \quad 0 \leq \tau < b \tag{D3}$$

Completing the derivation of Eq. 12.

Appendix E. Derivation of Eq. 19

Following the labeled cell derivation from Appendix A and Appendix C, let the number of cells removed at time T_{P1} be denoted by $N_{lab1}(t)$ and the number of cells removed at time T_{P2} be denoted by $N_{lab2}(t)$, then the total number of cells is given by:

$$N_{tot}(t) = N_{lab1}(t) + N_{lab2}(t) + N_{unlab}(t) \tag{E1}$$

where $N_{unlab}(t)$ is the number of unlabeled cells. Again, the interest is to quantify the number of unlabeled cells (i.e., cells not removed by the phlebotomies), which from Eq. E1 is given by:

$$N(t) \equiv N_{unlab}(t) = N_{tot}(t) - N_{lab1}(t) - N_{lab2}(t) \tag{E2}$$

From Eq. C1:

$$N_{tot}(t) = \int_{-\infty}^{t} f_{stim}(u) \cdot P_1(t - u) \cdot P_2(t - u, u)\, du \tag{E3}$$

and from Eq. C5:

$$N_{lab1}(t) = U(t - T_{P1}) \cdot [1 - F_1] \cdot \int_{-\infty}^{T_{P1}} f_{stim}(u) \cdot P_1(t - u) \cdot P_2(T_{P1} - u, u)\, du \tag{E4}$$

where $P_1(x)$ and $P_2(x, s)$ are defined as before (Appendix C). From Eq. C6 the total number of cells excluding cells labeled at time T_{P1} is given by:

$$\begin{aligned} N_{-lab1}(t) \equiv N_{tot}(t) - N_{lab1}(t) = & \int_{-\infty}^{t} f_{stim}(u) \cdot P_1(t - u) \cdot P_2(t - u, u)\, du \\ & - U(t - T_{P1}) \cdot [1 - F_1] \cdot \int_{-\infty}^{T_{P1}} f_{stim}(u) \\ & \cdot P_1(t - u) \cdot P_2(T_{P1} - u, u)\, du \end{aligned} \tag{E5}$$

From Eq. C2 through Eq. C4 it is realized that if the input of cells into the sampling space is stopped at time T_{P2} the first integrand in Eq. E5 is equal to:

$$\int_{-\infty}^{min(t,T_{P2})} f_{stim}(u) \cdot P_1(t - u) \cdot P_2(min(t, T_{P2}) - u, u)\, du \tag{E6}$$

giving:

$$\begin{aligned} N_{-lab1}(t) = & \int_{-\infty}^{min(t,T_{P2})} f_{stim}(u) \cdot P_1(t - u) \cdot P_2(min(t, T_{P2}) - u, u)\, du \\ & - U(t - T_{P1}) \cdot [1 - F_1] \cdot \int_{-\infty}^{T_{P1}} f_{stim}(u) \cdot P_1(t - u) \cdot P_2(T_{P1} - u, u)\, du \end{aligned} \tag{E7}$$

where Eq. E7 is equivalent to labeling all cells in the sampling space at time T_{P2} and counting the number of cells with the only the label given at time T_{P2}. Thus if only a fraction, $1 - F_2$, of the cells present at time T_{P2} are labeled (i.e., removed by the second phlebotomy) then the number of cells labeled at time T_{P2} is:

$$
\begin{aligned}
N_{lab2}(t) = {} & U(t - T_{P2}) \cdot [1 - F_2] \\
& \cdot \left[\begin{array}{l} \int_{-\infty}^{T_{P2}} f_{stim}(u) \cdot P_1(t-u) \cdot P_2(T_{P2} - u, u)\, du \\ -U(t - T_{P1}) \cdot [1 - F_1] \cdot \int_{-\infty}^{T_{P1}} f_{stim}(u) \cdot P_1(t-u) \cdot P_2(T_{P1} - u, u)\, du \end{array} \right] \\
= {} & U(t - T_{P2}) \cdot [1 - F_2] \cdot \int_{-\infty}^{T_{P2}} f_{stim}(u) \cdot P_1(t-u) \cdot P_2(T_{P2} - u, u)\, du \\
& -U(t - T_{P2}) \cdot [1 - F_2] \cdot [1 - F_1] \\
& \cdot \int_{-\infty}^{T_{P1}} f_{stim}(u) \cdot P_1(t-u) \cdot P_2(T_{P1} - u, u)\, du
\end{aligned} \tag{E8}
$$

Equations E2, E3, E4, and E8 give:

$$
\begin{aligned}
N(t) = {} & \int_{-\infty}^{t} f_{stim}(u) \cdot P_1(t-u) \cdot P_2(t - u, u)\, du \\
& -U(t - T_{P1}) \cdot [1 - F_1] \cdot \int_{-\infty}^{T_{P1}} f_{stim}(u) \cdot P_1(t-u) \cdot P_2(T_{P1} - u, u)\, du \\
& -U(t - T_{P2}) \cdot [1 - F_2] \cdot \int_{-\infty}^{T_{P2}} f_{stim}(u) \cdot P_1(t-u) \cdot P_2(T_{P2} - u, u)\, du \\
& + U(t - T_{P2}) \cdot [1 - F_2] \cdot [1 - F_1] \cdot \int_{-\infty}^{T_{P1}} f_{stim}(u) \cdot P_1(t-u) \cdot P_2(T_{P1} - u, u)\, du
\end{aligned} \tag{E9}
$$

Substitution of Eqs. C7 and C8 in Eq. E9 results in:

$$
\begin{aligned}
N(t) = {} & \int_{-\infty}^{t} f_{stim}(u) \cdot [1 - U(t - u - b)] \cdot \left[\int_{0}^{t-u} r(\omega, u)\, d\omega \right] du \\
& -U(t - T_{P1}) \cdot [1 - F_1] \cdot \int_{-\infty}^{T_{P1}} f_{stim}(u) \cdot [1 - U(t - u - b)] \\
& \cdot \left[\int_{0}^{T_{P1}-u} r(\omega, u)\, d\omega \right] du
\end{aligned}
$$

$$
\begin{aligned}
&-U\left(t-T_{P2}\right)\cdot\left[1-F_2\right]\cdot\int_{-\infty}^{T_{P2}} f_{stim}\left(u\right)\cdot\left[1-U\left(t-u-b\right)\right]\cdot\\
&\left[\int_0^{T_{P2}-u} r\left(\omega,u\right)d\omega\right]du\\
&+U\left(t-T_{P2}\right)\cdot\left[1-F_2\right]\cdot\left[1-F_1\right]\cdot\int_{-\infty}^{T_{P1}} f_{stim}\left(u\right)\cdot\left[1-U\left(t-u-b\right)\right]\\
&\cdot\left[\int_0^{T_{P1}-u} r\left(\omega,u\right)d\omega\right]du\\
=&\int_{t-b}^{t} f_{stim}\left(u\right)\cdot\left[\int_0^{t-u} r\left(\omega,u\right)d\omega\right]du-U\left(t-T_{P1}\right)\cdot\left[1-F_1\right]\\
&\cdot\int_{min(T_{P1},t-b)}^{T_{P1}} f_{stim}\left(u\right)\cdot\left[\int_0^{T_{P1}-u} r\left(\omega,u\right)d\omega\right]du\\
&-U\left(t-T_{P2}\right)\cdot\left[1-F_2\right]\cdot\int_{min(T_{P2},t-b)}^{T_{P2}} f_{stim}\left(u\right)\cdot\left[\int_0^{T_{P2}-u} r\left(\omega,u\right)d\omega\right]du\\
&+U\left(t-T_{P2}\right)\cdot\left[1-F_2\right]\cdot\left[1-F_1\right]\cdot\int_{min(T_{P1},t-b)}^{T_{P1}} f_{stim}\left(u\right)\\
&\cdot\left[\int_0^{T_{P1}-u} r\left(\omega,u\right)d\omega\right]du
\end{aligned}
\tag{E10}
$$

The unit step functions of the integrands are eliminated in the simplification step of Eq. E10 since it is recognized that the integrand will have a value of 0 at all times when $u < t-b$. However, by eliminating the units step functions the lower bound of the first integrals of the last three terms must then be constrained to be the $min\left(T_{Pi}, t-b\right)$, $i = 1, 2$, to maintain the integrals evaluation to zero at all values of $u < t-b$. This completes the derivation of Eq. 19.

Appendix F. Time variant Weibull distribution location parameter spline function

If we denote the nodes of the spline function by T_i $\left(T_{i+1} > T_i, i = 1, 2, \ldots, 8\right)$, the time variant Weibull distribution location parameter value, $\theta\left(t\right)$, was modeled as an end-constrained quadratic spline function as given by:

$$\theta(t) = S(t) \equiv S_i(t) \tag{F1}$$

where,

$$S_i(t) = \sum_{j=0}^{2} \alpha_{j,i} \cdot (t - T_i)^j, \quad T_i \le t < T_{i+1}, \quad i = 1, 2, \ldots, 7 \tag{F2}$$

Subject to continuity conditions on the function and its derivative:

$$S(T_i - \varepsilon) = S(T_i) \tag{F3}$$
$$S'(T_i - \varepsilon) = S'(T_i) \tag{F4}$$

and boundary constraints:

$$S(t) = S_1(T_1) \quad \text{for} \quad t < T_1 \equiv T_{P1} \tag{F5}$$

$$S(t) = S_7(T_8 - \varepsilon) \quad \text{for} \quad t \ge T_8 \le t_{last} \tag{F6}$$

where ε denotes an infinitely small time increment and t_{last} denotes the time of the last observation. Since for the Weibull distribution $\theta \ge 0$, the spline function was constrained to be non-negative by:

$$\theta(t) = \text{maximum}(\theta(t), 0) \tag{F7}$$

In all, 7 nodes and 6 unconstrained spline coefficients were estimated.

Appendix G. Derivation of equation for determining mean circulating reticulocyte lifespan (i.e., $E\{\mathrm{T}|s\}$)

The mean circulating reticulocyte lifespan is given by the $E\{\mathrm{T}|s\}$ taken with respect to the distribution given by Eq. 12, with $r(\cdot, s)$ as the fitted Weibull distribution. Therefore from Eq. 12 to Eq. 17:

$$\begin{aligned} E\{\mathrm{T}|s\} &= \frac{\int_0^b \tau \cdot r(b-\tau, s)\, d\tau}{\int_0^b r(\omega, s)\, d\omega} \\ &= \frac{\int_0^{b-\theta(s)} \tau \cdot \frac{k}{\lambda} \cdot \left[\frac{b-\tau-\theta(s)}{\lambda}\right]^{k-1} \cdot \exp\left(-\left[\frac{b-\tau-\theta(s)}{\lambda}\right]^k\right) d\tau}{\int_{\theta(s)}^b \frac{k}{\lambda} \cdot \left[\frac{\omega-\theta(s)}{\lambda}\right]^{k-1} \cdot \exp\left(-\left[\frac{\omega-\theta(s)}{\lambda}\right]^k\right) d\omega} \end{aligned} \tag{G1}$$

and by Eq. 18 the denominator of Eq. G1 becomes:

$$1 - \exp\left(-\left[\frac{b-\theta\,(s)}{\lambda}\right]^{k}\right) \quad \text{for} b \geq \theta\,(s) \text{ and 0 otherwise} \tag{G2}$$

If we define:

$$u = \left[\frac{b-\tau-\theta\,(s)}{\lambda}\right]^{k} \tag{G3}$$

Then by substitution of u into the numerator of Eq. G1, it becomes:

$$-\int_{\left[\frac{b-\theta(s)}{\lambda}\right]^{k}}^{0} \left[b-\theta\,(s)-\lambda\cdot u^{1/k}\right]\cdot\frac{k}{\lambda}\cdot\left[u^{1/k}\right]^{k-1}\cdot\exp\,(-u)\cdot\frac{\lambda\cdot u^{(1/k)-1}}{k}du \tag{G4}$$

which can be simplified to:

$$\begin{aligned}
&= \int_{0}^{\left[\frac{b-\theta(s)}{\lambda}\right]^{k}} \left[b-\theta\,(s)-\lambda\cdot u^{1/k}\right]\cdot u^{(k-1)/k}\cdot u^{(1-k)/k}\cdot\exp\,(-u)\,du \\
&= [b-\theta\,(s)]\cdot\int_{0}^{\left[\frac{b-\theta(s)}{\lambda}\right]^{k}} u^{(k-1+1-k)/k}\cdot\exp\,(-u)\,du - \lambda \\
&\quad\cdot\int_{0}^{\left[\frac{b-\theta(s)}{\lambda}\right]^{k}} \cdot u^{(k-1+1-k+1)/k}\cdot\exp\,(-u)\,du \\
&= [b-\theta\,(s)]\cdot\int_{0}^{\left[\frac{b-\theta(s)}{\lambda}\right]^{k}} \exp\,(-u)\,du - \lambda\cdot\int_{0}^{\left[\frac{b-\theta(s)}{\lambda}\right]^{k}} \cdot u^{1/k}\cdot\exp\,(-u)\,du \\
&= [b-\theta\,(s)]\cdot\left[1-\exp\left(-\left[\frac{b-\theta\,(s)}{\lambda}\right]^{k}\right)\right] - \lambda\cdot\gamma\left(1+1/k,\left[\frac{b-\theta\,(s)}{\lambda}\right]^{k}\right)
\end{aligned} \tag{G5}$$

where $\gamma\,(a,x)$ is the lower incomplete gamma function with integrand exponent parameter a and upper limit of the integral x. Dividing the numerator (Eq. G5) by

the denominator (Eq. G2) of Eq. G1 results in:

$$E\{\mathrm{T}|s\} = [b - \theta(s)] - \frac{\lambda \cdot \gamma\left(1 + 1/k, \left[\frac{b-\theta(s)}{\lambda}\right]^k\right)}{\left[1 - exp\left(-\left[\frac{b-\theta(s)}{\lambda}\right]^k\right)\right]} \quad \text{for } b > \theta(s) \qquad \text{(G6)}$$

Completing the derivation of $E\{\mathrm{T}|s\}$.

References

1. Dornhorst AC (1951) The interpretation of red cell survival curves. Blood 6:1284–1292
2. Callender ST, Powell EO, Witts LJ (1945) The life span of the red cell in man. J Pathol Bacteriol 57:129
3. Brown GM, Hayward OC, Powell EO, Witts LJ (1944) The destruction of transfused erythrocytes in anemia. J Pathol Bacteriol 56:81
4. Landaw SA (1988) Factors that accelerate or retard red blood cell senescence. Blood Cells 14:47–67
5. Hoffman R, Benz EJ Jr, Shattil SJ, Furie B, Cohen HJ, Silberstein LE, McGlave P (2005) Hematology: basic principles and applications, 4th edn. Elsevier Inc., United States of America
6. Brugnara C (2000) Reticulocyte cellular indices: a new approach in the diagnosis of anemias and monitoring of erythropoietic function. Crit Rev Clin Lab Sci 37:93–130
7. Hillman RS, Ault KA, Rinder HM (2005) Hematology in clinical practice, 4th edn. McGraw-Hill Companies Inc., United States of America
8. Harvey JW (2001) Atlas of veterinary hematology blood and bone marrow of domestic animals. W.B. Saunders Company, Philadelphia
9. Brugnara C (1998) Use of reticulocyte cellular indices in the diagnosis and treatment of hematological disorders. Int J Clin Lab Res 28:1–11
10. Jandl JH (1996) Blood: textbook of hematology, 2nd edn. Little, Brown and Company, United States of America
11. Houwen B (1992) Reticulocyte maturation. Blood Cells 18:167–186
12. Jain NC (1993) Essential of veterinary hematology. Lea & Febiger, Philadelphia
13. Friberg LE, Freijs A, Sandstrom M, Karlsson MO (2000) Semiphysiological model for the time course of leukocytes after varying schedules of 5-fluorouracil in rats. J Pharmacol Exp Ther 295:734–740
14. Veng-Pedersen P, Chapel S, Schmidt RL, Al-Huniti NH, Cook RT, Widness JA (2002) An integrated pharmacodynamic analysis of erythropoietin, reticulocyte, and hemoglobin responses in acute anemia. Pharm Res 19:1630–1635
15. Chapel SH, Veng-Pedersen P, Schmidt RL, Widness JA (2000) A pharmacodynamic analysis of erythropoietin-stimulated reticulocyte response in phlebotomized sheep. J Pharmacol Exp Ther 295:346–351
16. Krzyzanski W, Jusko WJ, Wacholtz MC, Minton N, Cheung WK (2005) Pharmacokinetic and pharmacodynamic modeling of recombinant human erythropoietin after multiple subcutaneous doses in healthy subjects. Eur J Pharm Sci 26:295–306
17. Ramakrishnan R, Cheung WK, Farrell F, Joffee L, Jusko WJ (2003) Pharmacokinetic and pharmacodynamic modeling of recombinant human erythropoietin after intravenous and subcutaneous dose administration in cynomolgus monkeys. J Pharmacol Exp Ther 306:324–331
18. Ramakrishnan R, Cheung WK, Wacholtz MC, Minton N, Jusko WJ (2004) Pharmacokinetic and pharmacodynamic modeling of recombinant human erythropoietin after single and multiple doses in healthy volunteers. J Clin Pharmacol 44:991–1002
19. Krzyzanski W, Ramakrishnan R, Jusko WJ (1999) Basic pharmacodynamic models for agents that alter production of natural cells. J Pharmacokinet Biopharm 27:467–489
20. Krzyzanski W, Perez-Ruixo JJ (2007) An assessment of recombinant human erythropoietin effect on reticulocyte production rate and lifespan distribution in healthy subjects. Pharm Res 24:758–772
21. Uehlinger DE, Gotch FA, Sheiner LB (1992) A pharmacodynamic model of erythropoietin therapy for uremic anemia. Clin Pharmacol Ther 51:76–89

22. Krzyzanski W, Woo S, Jusko WJ (2006) Pharmacodynamic models for agents that alter production of natural cells with various distributions of lifespans. J Pharmacokinet Pharmacodyn 33:125–166
23. Freise KJ, Widness JA, Schmidt RL, Veng-Pedersen P (2007) Pharmacodynamic analysis of time-variant cellular disposition: reticulocyte disposition changes in phlebotomized sheep. J Pharmacokinet Pharmacodyn 34:519–547
24. Kalbfeisch JD, Prentice RL (2002) The statistical analysis of failure time data, 2nd edn. Wiley, Hoboken, NJ
25. Grimes JM, Buss LA, Brace RA (1987) Blood volume restitution after hemorrhage in adult sheep. Am J Physiol 253:R541–R544
26. Widness JA, Veng-Pedersen P, Modi NB, Schmidt RL, Chestnut DH (1992) Developmental differences in erythropoietin pharmacokinetics: increased clearance and distribution in fetal and neonatal sheep. J Pharmacol Exp Therapeut 261:977–984
27. Veng-Pedersen P, Mandema JW, Danhof M (1991) A system approach to pharmacodynamics. III: an algorithm and computer program, COLAPS, for pharmacodynamic modeling. J Pharm Sci 80:488–495
28. Hutchinson MF, deHoog FR (1985) Smoothing noise data with spline functions. Numer Math 47:99–106
29. Mock DM, Lankford GL, Burmeister LF, Strauss RG (1997) Circulating red cell volume and red cell survival can be accurately determined in sheep using the [14C]cyanate label. Pediatr Res 41:916–921
30. Akaike H (1974) Automatic control: a new look at the statistical model identification. IEEE Trans 19:716–723
31. Veng-Pedersen P (1977) Curve fitting and modelling in pharmacokinetics and some practical experiences with NONLIN and a new program FUNFIT. J Pharmacokinet Biopharm 5:513–531
32. Piessens R, deDoncker-Kapenga E, Uberhuber CW, Kahaner DK (1983) QUADPACK. Springer-Verlag, New York
33. Holm S (1979) A simple sequentially rejective multiple test procedure.. Scand J Stat 6:65–70
34. Torrington KG, McNeil JS, Phillips YY, Ripple GR (1989) Blood volume determinations in sheep before and after splenectomy. Lab Anim Sci 39:598–602
35. Hillman RS (1969) Characteristics of marrow production and reticulocyte maturation in normal man in response to anemia. J Clin Invest 48:443–453
36. Shimada A (1975) The maturation of reticulocytes. II. Life-span of red cells originating from stress reticulocytes. Acta Med Okayama 29:283–289
37. Stohlman FJr (1961) Humoral regulation of erythropoiesis. VII. Shortened survival of erythrocytes produced by erythropoietine or severe anemia. Proc Soc Exp Biol Med 107:884–887
38. Al-Huniti NH, Widness JA, Schmidt RL, Veng-Pedersen P (2005) Pharmacodynamic analysis of changes in reticulocyte subtype distribution in phlebotomy-induced stress erythropoiesis. J Pharmacokinet Pharmacodyn 32:359–376
39. Harker LA, Roskos LK, Marzec UM, Carter RA, Cherry JK, Sundell B, Cheung EN, Terry D, Sheridan W (2000) Effects of megakaryocyte growth and development factor on platelet production, platelet life span, and platelet function in healthy human volunteers. Blood 95:2514–2522
40. Paulus JM (1971) Platelet kinetics: radioisotopic, cytological, mathematical, and clinical aspects. North-Holland Publishing Co., Amsterdam
41. Wiczling P, Krzyzanski W (2007) Method of determination of the reticulocyte age distribution from flow cytometry count by a structured-population model. Cytometry A 71:460–467

Glossary

$*$	Convolution operator
$1\{\cdot\}$	Indicator function
a, $a(s)$	Time invariant and time variant "point" cellular release time delay, respectively
AIC	Akaike's Information Criterion
b	Time from stimulation of a precursor cell to transformation into a new cell type or senescence/destruction of the subsequently released cell(s)
$C(t)$	Concentration

$C_{bio}(t)$	Biophase EPO concentration
$C_p(t)$	Plasma EPO concentration
Δ	Small time increment
$E\{\cdot\}$, $E\{\cdot\|\cdot\}$	Mathematical expectation and conditional expectation of a random variable, respectively
EC_{50}	C_{bio} that results in 50% of maximal erythrocyte stimulation rate
E_{max}	Maximal erythrocyte stimulation rate
EPO	Erythropoietin
ε	Infinitely small time increment
F, F_1, F_2	Fraction of cells remaining following a phlebotomy (subscript denotes phlebotomy number)
$f_{prod}(t)$	Production rate
$f_{stim}(t)$	Stimulation rate
k_{bio}	Biophase conduction function parameter
λ, k, and $\theta(t)$	Scale, shape, and time variant location parameters of the Weibull distribution, respectively
$\ell(\tau, \cdot)$	Time variant p.d.f. of cellular lifespans
$m(t)$	Subject mass (weight)
$MSE\%$	Mean percent standard error
$\mu_{RET,0}$	Mean initial (t_0) or baseline circulating reticulocyte lifespan
$\mu_{RET,MAX}$	Maximal circulating reticulocyte lifespan
$N(t)$	Number of cells
N_P, N_{P1}, N_{P2}	Number of cells removed by phlebotomy (subscript denotes phlebotomy number)
ω, Ω	Cellular release time delay, capital omega refers to random release time delay variable
PD	Pharmacodynamic
PK	Pharmacokinetic
$P(\cdot)$	Probability
p.d.f.	Probability density function
production	The physical input of cells into the sampling space
$r(\omega, s)$	Time variant p.d.f. of cellular release time delays
RBC	Red blood cell (may be sub-scripted with other terms)
RET	Reticulocyte (sub-scripted with other terms)
RNA	Ribonucleic acid
SD	Standard deviation
stimulation	Activation of cells prior to physical input into the sampling space
t	Time
t_0	Initial time
T_P, T_{P1}, T_{P2}	Time of phlebotomy (subscript denotes phlebotomy number)
τ, T	Cellular lifespan, i.e. the time from input into the sampling space to the time of output from the sampling space (capital tau refers to random cellular lifespan variable)
θ	Time invariant location parameter of the Weibull distribution
θ_0	Initial (t_0) location parameter value of the Weibull distribution

s	Time of stimulation
u	Arbitrary integration variable
$U(\cdot)$	Unit step function
$UR_\ell, UR_\ell(t, z)$	Time variant unit response defined by $\ell(\tau, z)$
$UR_r, UR_r(t, s)$	Time variant unit response defined by $r(\omega, s)$
V_n	Mass normalized constant total blood volume
$V(t)$	Total sampling space (blood) volume
$x(t)$	Time of stimulation of cells currently entering the sampling compartment using a "point distribution" cellular lifespan model
z	Time of production